



HAL
open science

A triazolium-anchored self-immolative linker enables self-assembly-driven siRNA binding and esterase-induced release

Selina Hollstein, Lamiaa Ali, Maëva Coste, Julian Vogel, Nadir Bettache, Sébastien Ulrich, Max von Delius

► To cite this version:

Selina Hollstein, Lamiaa Ali, Maëva Coste, Julian Vogel, Nadir Bettache, et al.. A triazolium-anchored self-immolative linker enables self-assembly-driven siRNA binding and esterase-induced release. *Chemistry - A European Journal*, 2023, 29 (8), pp.e202203311. 10.1002/chem.202203311 . hal-03854124

HAL Id: hal-03854124

<https://hal.science/hal-03854124>

Submitted on 23 Oct 2023

HAL is a multi-disciplinary open access archive for the deposit and dissemination of scientific research documents, whether they are published or not. The documents may come from teaching and research institutions in France or abroad, or from public or private research centers.

L'archive ouverte pluridisciplinaire **HAL**, est destinée au dépôt et à la diffusion de documents scientifiques de niveau recherche, publiés ou non, émanant des établissements d'enseignement et de recherche français ou étrangers, des laboratoires publics ou privés.



Distributed under a Creative Commons Attribution 4.0 International License

A Triazolium-Anchored Self-Immolative Linker Enables Self-Assembly-Driven siRNA Binding and Esterase-Induced Release

Selina Hollstein,^[a] Lamiaa M. A. Ali,^[b, c] Maëva Coste,^[b] Julian Vogel,^[a] Nadir Bettache,^[b] Sébastien Ulrich,^{*[b]} and Max von Delius^{*[a]}

Abstract: The increased importance of RNA-based therapeutics comes with a need to develop next-generation stimuli-responsive systems capable of binding, transporting and releasing RNA oligomers. In this work, we describe triazolium-based amphiphiles capable of siRNA binding and enzyme-responsive release of the nucleic acid payload. In aqueous medium, the amphiphile self-assembles into nanocarriers that can disintegrate upon the addition of esterase. Key to the molecular design is a self-immolative linker that is anchored to the triazolium moiety and acts as a positively-charged

polar head group. We demonstrate that addition of esterase leads to a degradation cascade of the linker, leaving the neutral triazole compound unable to form complexes and therefore releasing the negatively-charged siRNA. The reported molecular design and overall approach may have broad utility beyond this proof-of-principle study, because the underlying CuAAC “click” chemistry allows bringing together three groups very efficiently as well as cleaving off one of the three groups under the mild action of an esterase enzyme.

Introduction

After a bumpy road paved with hopes and failures, patients can today benefit from small interfering RNA (siRNA) drugs^[1,2] and messenger RNA (mRNA) vaccines.^[3,4] In 2018, the first-of-its-kind siRNA-based drug Patisiran was FDA-approved, followed by three other RNA interference-based therapeutics in 2019, 2020 and 2021 (Givosiran, Lumasiran, Inclisiran).^[5,6] In 2020, the FDA granted an emergency use authorization of mRNA vaccines to fight the Covid-19 pandemic,^[7] and further RNA-based drugs are currently in clinical trials.^[8,9]

The success of these RNA-based therapeutics relies largely on the development of lipid nanoparticle nanovectors such as

micelleplexes^[10–13] and liposomes^[14–17] which protect RNAs from enzymatic degradation by nucleases, while also promoting (targeted) cell internalization.^[18–23] The composition of those FDA-approved four-component (lipid-PEG, helper lipid, cholesterol, ionizable lipid) nanoparticles is crucial for effective cell delivery. In particular, the nature of the ionizable lipid has been optimized to greatly improve their delivery efficacy through an enhancement in endosomal escape – two-armed cylindrical or inverted cone structures with packing parameter greater than 1/2 being a must.^[24–27]

However, these multi-component formulations must be preserved at (ultra)low temperatures for storage and distribution to preserve their structure (current limit of 1–3 months at 2–8 °C for the mRNA Covid-19 vaccines^[28,29]). Therefore, a current challenge in the field is to make these lipid nanoparticles more stable while keeping their dynamic nature which is key to deliver the nucleic acid payload. In other works, self-assembly has to be dynamically expressed, turned on to stabilize nucleic acid complexes and turned off to trigger nucleic acid release.^[30–34] In this line, the development of responsive systems is of current interest for the next generation of lipid nanoparticles.

Several reports aimed at addressing this challenge, in particular through the design of i) biodegradable lipid nanoparticles that degrade at the acidic pH found in late endosomes or in the intracellular reductive environment,^[35–39] or ii) pH-responsive switchable lipids.^[40–43] In addition to these endogenous pH and redox effectors, enzymes also represent a trigger of choice for controlled drug delivery.^[44–46] Hitherto, a limited number of cases have reported on enzyme-responsive RNA delivery using peptide conjugates,^[47] modified siRNA,^[48] and ester-based amphiphilic dendrimers.^[49]

[a] S. Hollstein, J. Vogel, Prof. Dr. M. von Delius
Institute of Organic Chemistry
Ulm University
Albert-Einstein-Allee 11, 89081 Ulm (Germany)
E-mail: max.vondelius@uni-ulm.de

[b] Dr. L. M. A. Ali, Dr. M. Coste, Dr. N. Bettache, Dr. S. Ulrich
Institut des Biomolécules Max Mousseron (IBMM)
CNRS, Université de Montpellier, ENSCM
Montpellier (France)
E-mail: sebastien.ulrich@cnrs.fr

[c] Dr. L. M. A. Ali
Department of Biochemistry
Medical Research Institute
University of Alexandria
21561 Alexandria (Egypt)

Supporting information for this article is available on the WWW under <https://doi.org/10.1002/chem.202203311>

© 2022 The Authors. Chemistry - A European Journal published by Wiley-VCH GmbH. This is an open access article under the terms of the Creative Commons Attribution License, which permits use, distribution and reproduction in any medium, provided the original work is properly cited.

Herein, we report the synthesis of amphiphiles with positively charged triazolium head groups that self-assemble into vesicular structures and are able to complex siRNA. After addition of a stimulus (here: esterase) the polar head group of the amphiphiles degrades irreversibly by forming a neutral triazole and siRNA gets released.

Results and Discussion

Design of amphiphiles and aggregation behavior

A wide range of self-immolative linkers have been used in stimuli-responsive drug delivery systems.^[44,50–52] Whereas most known self-immolative linkers are bound to functional groups such as the hydroxy or amine moiety,^[53–56] functionalization of a triazole moiety is rare^[57,58] and the strategic use of a triazolium group is elusive. We reasoned that the triazole is a promising anchor for self-immolative groups, because 1) it can be generated in a modular way by CuAAC “click” chemistry, thus enabling the introduction of different (lipid) chains; 2) the conversion of triazoles to triazolium motifs is accompanied with the introduction of a positive charge, enabling subsequent amphiphilic self-assembly and concomitant complexation of

negatively-charged (bio)molecules such as nucleic acids; 3) upon addition of a certain stimulus, the self-immolative linker would degrade, leaving the neutral triazole unable to self-assemble and complex the nucleic acid, thereby triggering its controlled release (Figure 1a).

The first consideration when designing the specific self-immolative linker was the choice of a stimulus for its cleavage. We decided to use porcine liver esterase as trigger due to its commercial availability and overexpression of esterases in cancer cells.^[59,60] A benzyl pivalate linker was used (Figure 1b), because its background hydrolysis is negligible in aqueous medium (pH 7.2, phosphate buffered saline (PBS)), while its cleavage has been documented in vitro.^[53] Cleavage of the ester bond would result in the release of pivalic acid, followed by a degradation cascade during which quinone methide and the triazole are formed. Quinone methide as a strong Michael acceptor reacts rapidly with water to give 4-hydroxybenzyl alcohol.

We therefore synthesized three compounds with the same head group, but with varying tails. Overall, our amphiphiles feature a permanent cationic head and two lipophilic chains. We combined tails with different chain lengths (C_6 , C_8 , C_{12} or C_{14}) containing either one or no unsaturated bond, resulting in three compounds: C_6TC_6 , C_8TC_{12} and $C_{14}TC_{12}$ (Figure 1b).

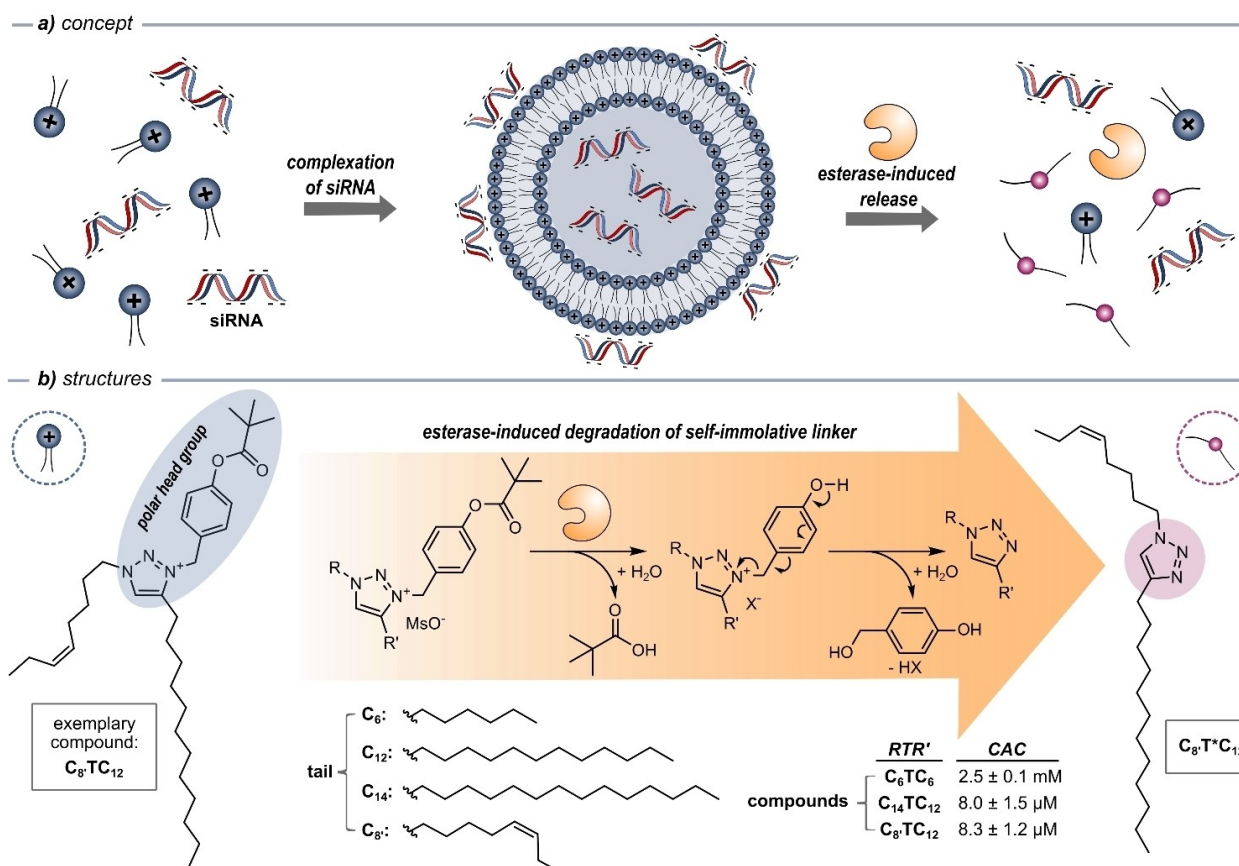


Figure 1. a) Self-assembly-based siRNA binding and esterase-induced siRNA release via cleavage of amphiphiles. b) Structures of triazolium-based amphiphiles, and proposed cleavage mechanism resulting in the formation of neutral triazoles. Compounds were synthesized with a mesylate (MsO^-) counterion, but rapid ion exchange occurs in the buffer (X^-). The critical aggregation concentrations (CAC) were determined using fluorescence spectroscopy with the fluorescent dye 1,6-diphenyl-1,3,5-hexatriene, which shows aggregation-caused quenching.

To study the aggregation behavior of the compounds, the critical aggregation concentration (CAC) was determined (Figure 1b and Figure S1). Therefore, the fluorescent dye 1,6-diphenyl-1,3,5-hexatriene (DPH) was added to different concentrations of each compound in PBS. This nonpolar dye shows aggregation-caused quenching in aqueous media, while its photoluminescence increases in a non-linear way, if the dye is incorporated into a lipophilic nanoenvironment. The CAC of the compound containing the shortest hydrophobic tails (C_6TC_6) exhibited the highest CAC (2.5 ± 0.1 mM), which we deemed too high for the purposes of drug delivery. Due to their longer hydrophobic tails, compounds C_8TC_{12} and $C_{14}TC_{12}$ did however show CACs three orders of magnitude lower (8.3 ± 1.2 μ M and 8.0 ± 1.5 μ M, respectively), which is why we pursued these two compounds further. The addition of siRNA ($N/P = 10$, see below) did not have a pronounced effect on the CAC (Table S1).

Dynamic light scattering (DLS) was performed to obtain the average size of the aggregates, and ζ -potential measurements indicated on the surface charge of those nanoassemblies. Solutions of the compounds in PBS at concentrations higher than the CAC (30 μ M) revealed nanoassemblies with a hydrodynamic diameter of 173 ± 25 and 185 ± 5 nm and ζ -potentials of 35.0 ± 5.6 and 33.4 ± 3.3 mV, for C_8TC_{12} and $C_{14}TC_{12}$, respectively.

The aggregation of compounds C_8TC_{12} (210 μ M) and $C_{14}TC_{12}$ (300 μ M) into spherical assemblies with diameters of 140–280 nm (C_8TC_{12} ; presumably liposomes) and 160–375 nm ($C_{14}TC_{12}$) was confirmed by transmission electron microscopy (TEM) (Figure 3a and Figure S2). Confocal fluorescence microscopy using a lipophilic styryl membrane dye showed, at concentrations of 300 μ M in Dulbecco's Modified Eagle Medium (DMEM), the formation of spherical aggregates of average diameter around 900 nm for C_8TC_{12} and somewhat larger, less well-defined aggregates for $C_{14}TC_{12}$ (Figure S3). Further, $C_{14}TC_{12}$ showed less ability to be stained compared to C_8TC_{12} . It needs to be noted that the average size of the nanocarriers lies below the detection limit of optical microscopy and therefore the consistent DLS and TEM data are more reliable regarding (average) size.

Complexation of siRNA

The ability of the nanoassemblies of amphiphilic triazolium compounds to complex siRNA was assessed by gel electrophoresis. Each compound was mixed with a fixed amount of siRNA (0.5 μ M) at different N/P ratios (molar ratio of positively-charged triazolium nitrogen atoms per negatively-charged phosphodiester in siRNA). The final concentration of the triazolium compounds ranged from 21 to 210 μ M for C_8TC_{12} and $C_{14}TC_{12}$ (above the CAC) and from 210 to 840 μ M for C_6TC_6 (below the CAC). Both C_8TC_{12} and $C_{14}TC_{12}$ showed partial complexation of siRNA at $N/P = 5$ and a complete complexation was found at $N/P = 10$ (Figure 2). On the other hand, C_6TC_6 only showed partial complexation of siRNA up to $N/P = 40$ (Figure 2). In this case the concentration of the compound is below the CAC, thus no assemblies are formed. From this result which

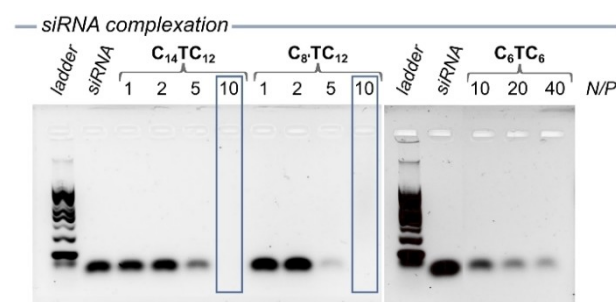


Figure 2. Gel electrophoresis of siRNA complexation by $C_{14}TC_{12}$ (left), C_8TC_{12} (middle) and C_6TC_6 (right) in the presence of siRNA (0.5 μ M, $N/P = 1, 2, 5, 10, 20$ and 40). The blue box highlights the runs with full complexation.

demonstrated siRNA complexation by the positively-charge nanoassemblies of the amphiphilic triazoliums, we selected C_8TC_{12} and $C_{14}TC_{12}$ as the best compounds to move forward.

DLS and ζ -potential analyses showed nanoassemblies formed at $N/P = 10$ with hydrodynamic diameters of 182 ± 36 and 184 ± 25 nm, and ζ -potentials of 34.3 ± 4.7 and 25.3 ± 4.2 mV, for C_8TC_{12} and $C_{14}TC_{12}$ (see below), thereby indicating that siRNA complexation has little effect on the size and surface charge of the nanoassemblies, suggesting that the load preferentially fills their inner volume which is predetermined by the amphiphilic self-assembly of the triazolium compounds. In support of this conclusion, the determination of the CAC in presence of siRNA showed no changes (Figure S1), confirming the absence of any templating role of the siRNA in this case.

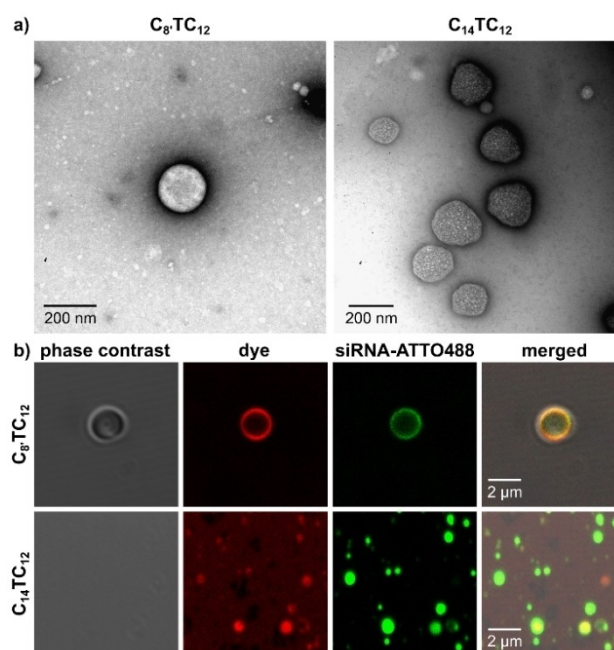


Figure 3. a) Transmission electron microscopy (TEM) images of C_8TC_{12} (210 μ M) and $C_{14}TC_{12}$ (300 μ M) after negative staining with $UO_2(OAc)_2$. b) Microscopy imaging of C_8TC_{12} and $C_{14}TC_{12}$ (300 μ M) complexed with 0.1 μ M siRNA-ATTO488, then stained with lipophilic styryl dye.

The morphologies of the siRNA complexes were visualized by confocal fluorescence microscopy using a fluorophore-labeled siRNA (Figure 3b). No significant difference in size was observed when the C_8TC_{12} aggregates were treated with labelled siRNA. Striking differences in the complexation mode of siRNA were detected, however, between C_8TC_{12} and $C_{14}TC_{12}$, with superficial binding dominating with C_8TC_{12} (suggesting liposome structure) and internal binding occurring with $C_{14}TC_{12}$ (suggesting nanoparticle structure).

Esterase-induced disassembly and release of siRNA

To study the esterase-induced conversion of the triazolium to the triazole compounds, we performed the degradation reaction using C_8TC_{12} and $C_{14}TC_{12}$ in the absence and presence of esterase. We chose porcine liver esterase (4 Units per μmol triazolium), PBS buffer (pH 7.2) as solvent, and the temperature was set to 37°C . After four hours, the organic compounds were extracted from the aqueous phase using ethyl acetate and a ^1H NMR spectrum was recorded after removal of the solvent (Figure 4). Fortunately, in the absence of esterase no hydrolysis of the ester bond was detected, implying that both triazolium compounds are hydrolytically stable in aqueous medium.

Upon addition of esterase, however, new peaks occurred in the ^1H NMR spectrum of C_8TC_{12} . The most pronounced shift was observed for the signal belonging to the triazolium/triazole proton from 9.82 (*a*) to 7.23 (*a'*) ppm. Additionally, the signal of the benzyl moiety (*b*) at 5.67 ppm decreased and a new peak at 4.61 ppm arose, which can be attributed to the formation of 4-hydroxybenzyl alcohol (*b'*). The ratio between triazolium C_8TC_{12} and triazole $C_8T^*C_{12}$ appears to be 15:85 – hence an 85% conversion of the enzymatic reaction is deduced. It should be noted, that a full conversion is not necessarily needed to realize our release concept, because any concentration of

residual triazolium below the CAC will lead to disintegration of the aggregates. When the reaction was performed using $C_{14}TC_{12}$, only a conversion of around 8% was observed, even when the reaction was run for 24 h (Figure S4). In light of the kinetic profile observed by NMR spectroscopy, gel electrophoresis and ethidium bromide displacement assay (see below), we propose that the triazole compound $C_{14}T^*C_{12}$ with longer tails leads to product inhibition. Notably, in all four reactions the signal corresponding to the triazolium proton shows a slight shift compared to the starting material (Figure S21 and Figure S27) due to counterion exchange during the reaction. In all cases, the signal corresponding to the methyl group of the mesylate counterion has disappeared (in essence, MsO^- is replaced with a large variety of different anions present in the buffer).

The kinetics of esterase-induced release of the siRNA was also studied by gel electrophoresis. The complexes of C_8TC_{12} and $C_{14}TC_{12}$ with siRNA (N/P=10) were treated with esterase (4 U/ μmol) and incubated at 37°C for different time intervals. After four hours, only a weak siRNA release was observed when using $C_{14}TC_{12}$. However, in the case of C_8TC_{12} a complete release of siRNA was reached already after 30 minutes (Figure 5). These results are consistent with the data obtained by ^1H NMR experiments. As explained previously, a complete conversion to the neutral triazole is not crucial for complete siRNA release. The concentration of residual triazolium only needs to decrease below the CAC, while the conversion of the triazolium into triazole lowers the N/P ratio, which also contributes to siRNA release.

siRNA complexation and release were further studied by a fluorescence displacement assay with ethidium bromide (EthBr). The dye shows high fluorescence emission at 590 nm upon intercalation into siRNA. The addition of an siRNA complexing agent leads to a decrease of the emission due to the expulsion of EthBr. A dimethyl sulfoxide (DMSO) solution of compound C_8TC_{12} or $C_{14}TC_{12}$ (21 mM) was added to a solution of siRNA (0.5 μM) and EthBr (5 μM) in PBS to obtain a final concentration of the triazolium compounds of 210 μM (above CAC). A significant decrease of the fluorescence emission intensity was observed over a period of three hours, when the compounds were added as a DMSO solution (Figure 6). When changing the

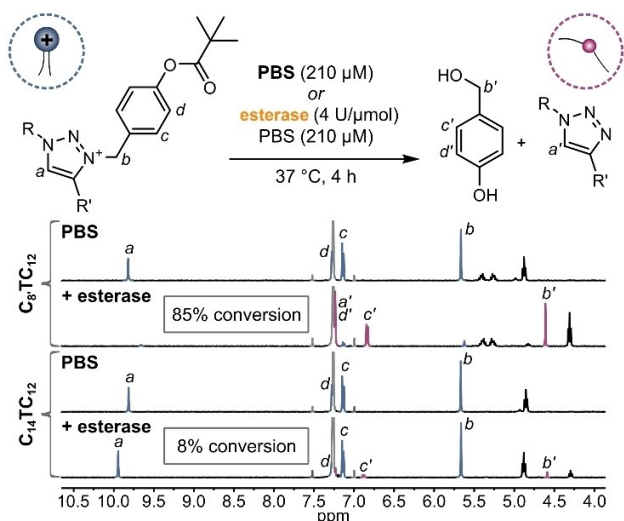


Figure 4. ^1H NMR stacked plot of products after stirring compounds C_8TC_{12} (top) and $C_{14}TC_{12}$ (bottom) at 37°C for four hours in the absence (upper) or in the presence of esterase (lower).

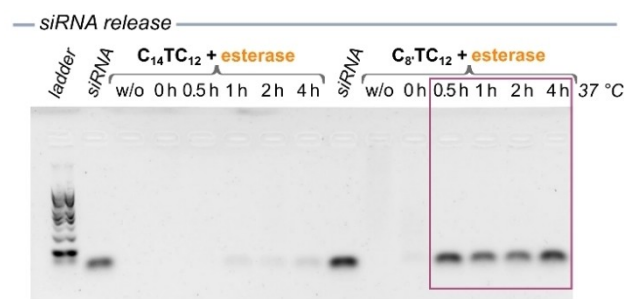


Figure 5. Gel electrophoresis of kinetic monitoring of siRNA release by $C_{14}TC_{12}$ (left) and C_8TC_{12} (right) in the presence of esterase (4 U/ μmol) after 0, 0.5, 1, 2 and 4 h (N/P = 10). The purple box highlights the runs with complete siRNA release.

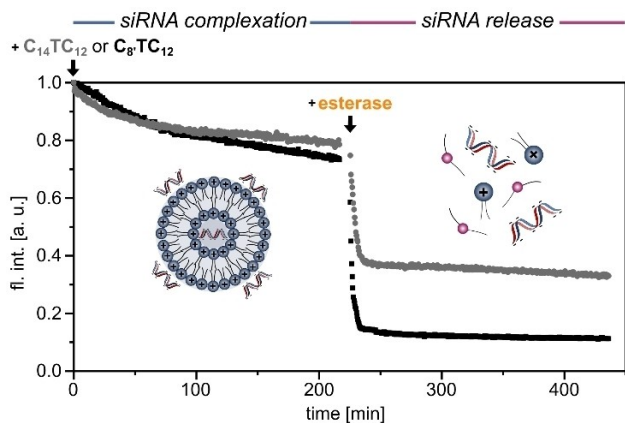


Figure 6. Kinetic monitoring of the fluorescence (590 nm) of an ethidium bromide/siRNA complex (5 μM and 0.5 μM in PBS buffer, respectively) after the addition of compound C_8TC_{12} or $\text{C}_{14}\text{TC}_{12}$ (210 μM , N/P = 10, addition as DMSO solution) at room temperature ($T = 0$ min). After 225 min, the spectrometer was heated to 37 $^\circ\text{C}$ and esterase (4 U/ μmol) was added to monitor the kinetics of siRNA release.

order of addition and omitting DMSO as a solvent, i.e. siRNA was added to a solution of compound C_8TC_{12} or $\text{C}_{14}\text{TC}_{12}$ and EthBr in PBS, the formation of the complex between the nanoassemblies and siRNA appeared to be much faster (Figure S6). Hence, when DMSO is used as a solvent, the rate of either nanoparticle assembly or siRNA complexation is slowed down. In these assays, we observed no pronounced difference in the complexation ability between compounds C_8TC_{12} and $\text{C}_{14}\text{TC}_{12}$, which is in line with the results obtained by gel electrophoresis (see above).

In contrast, differences between both compounds were found when studying siRNA release. Even though the kinetics of siRNA release were almost identical in both reactions (complexation after 15 minutes), the outcome was different. The decrease of fluorescence intensity was much more pronounced with C_8TC_{12} . Of note, typically an intensity increase would be expected in such an assay, because the release of siRNA should lead to regeneration of the EthBr/siRNA complex. We propose that our finding of decreased emission upon siRNA release is due to the precipitation of the triazole products $\text{C}_8\text{T}^*\text{C}_{12}$ and $\text{C}_{14}\text{T}^*\text{C}_{12}$ which could remove the EthBr dye effectively from the solution (Figure S8). Given the molecular structures, it is reasonable to assume that the flat EthBr dye would coprecipitate with the triazole compounds. As a control experiment, we measured the fluorescence of the EthBr/siRNA complex in the absence of the amphiphile and found that the intensity was not changing when adding esterase to the complex (Figure S5). Overall, the EthBr assay is valuable as a complement to gel electrophoresis, because it shows in *real time* that siRNA release is completed after 15 to 30 minutes. Such a kinetic profile is of interest, because it matches the process of maturation of endosomes in endocytotic cell penetration.^[61]

To complete this proof-of-principle study, the esterase-induced transformations were monitored by DLS and ζ -

potential measurements (Table 1). After incubation at 37 $^\circ\text{C}$ for four hours, the samples were filtered to remove any precipitate. In the case of C_8TC_{12} , DLS showed a strong decrease in size (hydrodynamic diameter of 2.1 ± 0.4 nm) along with negligible ζ -potential (-1.03 ± 0.97 mV), which is in agreement with the 85% enzymatic transformation of the cationic triazolium into the neutral triazole $\text{C}_8\text{T}^*\text{C}_{12}$ (entry 3, Table 1). The slight negative potential is almost within error and may be explained by the background ζ -potential of the buffer (Table S3). This result shows, that even without full degradation of the triazolium compounds, the residual amphiphiles are not able to form aggregates. In contrast, when studying $\text{C}_{14}\text{TC}_{12}$ only minor changes are observed by DLS (entry 7, Table 1), which is in agreement with the low conversion of $\text{C}_{14}\text{TC}_{12}$ observed by NMR spectroscopy. Crucially, the same trends were found when esterase and siRNA (at N/P = 10) were added to the pre-assembled aggregates, thus confirming that only amphiphile C_8TC_{12} undergoes effective esterase-induced disassembly and therefore allows the release of siRNA.

Conclusion

We report the design of a new type of amphiphile that is accessible via CuAAC “click” reaction and features a positively charged triazolium head group capable of the formation of self-assembled nanocarriers and thereby the complexation of siRNA. At the polar head group, a self-immolative linker is attached to a triazolium moiety in such a way that addition of esterase leads to the formation of a neutral triazole compound that is unable to form aggregates and therefore releases the siRNA load. Whereas one specific compound (C_6TC_6) showed a CAC too high to be relevant in drug delivery, two other compounds (C_8TC_{12} and $\text{C}_{14}\text{TC}_{12}$) exhibited micromolar CACs and were therefore studied in more detail. While both compounds showed similar siRNA complexation behavior, the siRNA release was much more efficient for compound C_8TC_{12} . We propose that the reason for this finding is that the two long aliphatic

Table 1. Particle size, polydispersity index (PDI) and ζ -potential characterization by dynamic light scattering and ζ -potential measurements of C_8TC_{12} and $\text{C}_{14}\text{TC}_{12}$ after the addition of siRNA and/or esterase in PBS buffer.

Entry	Compounds	Size \pm SD [nm]	PDI \pm SD	ζ -potential \pm SD [mV] ^[d]
1	C_8TC_{12} ^[a]	173 ± 25	0.31 ± 0.04	35.0 ± 5.6
2	+ only siRNA ^[b]	182 ± 36	0.25 ± 0.07	34.3 ± 4.7
3	+ only esterase ^[c]	2.1 ± 0.4	0.62 ± 0.10	-1.03 ± 0.97
4	+ siRNA + esterase ^[c]	2.4 ± 2.9	0.67 ± 0.08	-2.21 ± 1.93
5	$\text{C}_{14}\text{TC}_{12}$ ^[a]	185 ± 5	0.26 ± 0.04	33.4 ± 3.3
6	+ only siRNA ^[b]	184 ± 25	0.37 ± 0.06	25.3 ± 4.2
7	+ only esterase ^[c]	241 ± 49	0.35 ± 0.11	26.6 ± 4.5
8	+ siRNA + esterase ^[c]	189 ± 19	0.36 ± 0.01	11.3 ± 2.8

[a] triazolium at concentration of 30 μM . [b] N/P = 10, incubation at room temperature for five hours. [c] 4 U/ μmol , incubation at 37 $^\circ\text{C}$ for four hours. [d] measured in triplicate to rule out error caused by degradation of electrodes by PBS. SD = standard deviation.

chains in the lipophilic product $C_{14}T^*C_{12}$ lead to product inhibition, for instance via persistent binding to the esterase's active site. Product inhibition on the same magnitude was not observed for compound C_8TC_{12} , in which one aliphatic chain is only roughly half as long (C_8 vs. C_{14}). This delivery system may therefore allow the selective release of siRNA in cells showing a high concentration of esterase, for example in cancer cells. Future work will focus on mixed compositions with additional phospholipids, fine-tuning of lipophilicity and in vitro studies.

Acknowledgements

We thank the French Ministère de l'Europe et des Affaires étrangères (MEAE) and the French Ministère de l'Enseignement supérieur, de la Recherche et de l'Innovation (MESRI) for a Partenariat Hubert Curien (PHC Procope 42522SH). S.H. and M.v.D. thank the DAAD (German Academic Exchange Service) for a PPP mobility grant. M.v.D. acknowledges support by the European Union (ERCstg 802428 "SUPRANET"). S.U. thanks the ANR (ANR-17-CE07-0042-01) for funding. We acknowledge the Montpellier RIO Imaging platform (ANR-10-INBS-04), member of FranceBioImaging, for access to imaging facilities. Open Access funding enabled and organized by Projekt DEAL.

Conflict of Interest

The authors declare no conflict of interest.

Data Availability Statement

The data that support the findings of this study are available in the supplementary material of this article.

Keywords: amphiphiles · click chemistry · drug delivery · self-assembly · siRNA delivery

- [1] H. Ledford, *Nature* **2018**, *560*, 291–292.
- [2] E. C. Hayden, *Nature* **2014**, *508*, 443.
- [3] B. Baptista, R. Carapito, N. Laroui, C. Pichon, F. Sousa, *Pharmaceutica* **2021**, *13*, 2090.
- [4] N. Pardi, M. J. Hogan, F. W. Porter, D. Weissman, *Nat. Rev. Drug Discovery* **2018**, *17*, 261–279.
- [5] B. Hu, L. Zhong, Y. Weng, L. Peng, Y. Huang, Y. Zhao, X. J. Liang, *Signal Transduct. Target. Ther.* **2020**, *5*, 101.
- [6] L. M. A. Ali, M. Gary-Bobo, *Cancers* **2022**, *14*, 3597.
- [7] R. Verbeke, I. Lentacker, S. C. De Smedt, H. Dewitte, *J. Controlled Release* **2021**, *333*, 511–520.
- [8] S. M. Hammond, A. Aartsma-Rus, S. Alves, S. E. Borgos, R. A. M. Buijsen, R. W. J. Collin, G. Covello, M. A. Denti, L. R. Desviat, L. Echevarria, C. Foged, G. Gaina, A. Garanto, A. T. Goyenvalle, M. Guzowska, I. Holodnuka, D. R. Jones, S. Krause, T. Lehto, M. Montolio, W. Van Roon-Mom, V. Arechavala-Gomez, *EMBO Mol. Med.* **2021**, *13*, e13243.
- [9] K. Servick, *Science* **2020**, *370*, 1388–1390.
- [10] Z. Tan, Y. Jiang, W. Zhang, L. Karls, T. P. Lodge, T. M. Reineke, *J. Am. Chem. Soc.* **2019**, *141*, 15804–15817.
- [11] M. Pereira-Silva, I. Jarak, C. Alvarez-Lorenzo, A. Concheiro, A. C. Santos, F. Veiga, A. Figueiras, *J. Controlled Release* **2020**, *323*, 442–462.

- [12] T. M. Sun, J. Z. Du, Y. D. Yao, C. Q. Mao, S. Dou, S. Y. Huang, P. Z. Zhang, K. W. Leong, E. W. Song, J. Wang, *ACS Nano* **2011**, *5*, 1483–1494.
- [13] C. Wang, X. Wang, L. Du, Y. Dong, B. Hu, J. Zhou, Y. Shi, S. Bai, Y. Huang, H. Cao, Z. Liang, A. Dong, *ACS Appl. Mater. Interfaces* **2021**, *13*, 2218–2229.
- [14] C. R. Safinya, K. K. Ewert, R. N. Majzoub, C. Leal, *New J. Chem.* **2014**, *38*, 5164–5172.
- [15] Z. Gu, C. G. Da Silva, K. van der Maaden, F. Ossendorp, L. J. Cruz, *Pharmaceutica* **2020**, *12*, 1054.
- [16] Y. Li, H. Cong, S. Wang, B. Yu, Y. Shen, *Biomater. Sci.* **2020**, *8*, 6442–6468.
- [17] M. Nazir Hossen, L. Wang, H. R. Chinthalapally, J. D. Robertson, K. M. Fung, S. Wilhelm, M. Bieniasz, R. Bhattacharya, P. Mukherjee, *Sci. Adv.* **2020**, *6*, eaba5379.
- [18] Y. Eygeris, M. Gupta, J. Kim, G. Sahay, *Acc. Chem. Res.* **2022**, *55*, 2–12.
- [19] K. Paunovska, D. Loughrey, J. E. Dahlman, *Nat. Rev. Genet.* **2022**, *23*, 265–280.
- [20] Y. Zhang, C. Sun, C. Wang, K. E. Jankovic, Y. Dong, *Chem. Rev.* **2021**, *121*, 12181–12277.
- [21] X. Hou, T. Zaks, R. Langer, Y. Dong, *Nat. Rev. Mater.* **2021**, *6*, 1078–1094.
- [22] M. D. Buschmann, M. J. Carrasco, S. Alshetty, M. Paige, M. G. Alameh, D. Weissman, *Vaccine* **2021**, *9*, 65.
- [23] S. Yonezawa, H. Koide, T. Asai, *Adv. Drug Delivery Rev.* **2020**, *154–155*, 64–78.
- [24] X. Han, H. Zhang, K. Butowska, K. L. Swingle, M. G. Alameh, D. Weissman, M. J. Mitchell, *Nat. Commun.* **2021**, *12*, 8–13.
- [25] M. Jayaraman, S. M. Ansell, B. L. Mui, Y. K. Tam, J. Chen, X. Du, D. Butler, L. Eltepu, S. Matsuda, J. K. Narayanannair, K. G. Rajeev, I. M. Hafez, A. Akinc, M. A. Maier, M. A. Tracy, P. R. Cullis, T. D. Madden, M. Manoharan, M. J. Hope, *Angew. Chem. Int. Ed.* **2012**, *51*, 8529–8533; *Angew. Chem.* **2012**, *124*, 8657–8661.
- [26] S. C. Semple, A. Akinc, J. Chen, A. P. Sandhu, B. L. Mui, C. K. Cho, D. W. Y. Sah, D. Stebbing, E. J. Crosley, E. Yaworski, I. M. Hafez, J. R. Dorkin, J. Qin, K. Lam, K. G. Rajeev, K. F. Wong, L. B. Jeffs, L. Nechev, M. L. Eisenhardt, M. Jayaraman, M. Kazem, M. A. Maier, M. Srinivasulu, M. J. Weinstein, Q. Chen, R. Alvarez, S. A. Barros, S. De, S. K. Klimuk, T. Borland, V. Kosovrasti, W. L. Cantley, Y. K. Tam, M. Manoharan, M. A. Ciufolini, M. A. Tracy, A. De Fougerolles, I. MacLachlan, P. R. Cullis, T. D. Madden, M. J. Hope, *Nat. Biotechnol.* **2010**, *28*, 172–176.
- [27] M. Schlich, R. Palomba, G. Costabile, S. Mizrahy, M. Pannuzzo, D. Peer, P. Decuzzi, *Bioeng. Transl. Med.* **2021**, *6*, e10213.
- [28] L. Taina-González, M. de la Fuente, *Pharmaceutica* **2022**, *14*, 460.
- [29] L. Schoenmaker, D. Witzigmann, J. A. Kulkarni, R. Verbeke, G. Kersten, W. Jiskoot, D. J. A. Crommelin, *Int. J. Pharm.* **2021**, *601*, 120586.
- [30] D. K. Smith, *Chem. Commun.* **2018**, *54*, 4743–4760.
- [31] A. Barnard, D. K. Smith, *Angew. Chem. Int. Ed.* **2012**, *51*, 6572–6581; *Angew. Chem.* **2012**, *124*, 6676–6685.
- [32] Z. Lyu, L. Ding, A. Tintaru, L. Peng, *Acc. Chem. Res.* **2020**, *53*, 2936–2949.
- [33] S. Ulrich, *Acc. Chem. Res.* **2019**, *52*, 510–519.
- [34] E. Bartolami, Y. Bessin, V. Gervais, P. Dumy, S. Ulrich, *Angew. Chem. Int. Ed.* **2015**, *54*, 10183–10187; *Angew. Chem.* **2015**, *127*, 10321–10325.
- [35] M. Qiu, Y. Li, H. Bloomer, Q. Xu, *Acc. Chem. Res.* **2021**, *54*, 4001–4011.
- [36] L. Miao, J. Lin, Y. Huang, L. Li, D. Delcassian, Y. Ge, Y. Shi, D. G. Anderson, *Nat. Commun.* **2020**, *11*, 2424.
- [37] H. Tanaka, N. Takata, Y. Sakurai, T. Yoshida, T. Inoue, S. Tamagawa, Y. Nakai, K. Tange, H. Yoshioka, M. Maeki, M. Tokeshi, H. Akita, *Pharmaceutica* **2021**, *13*, 544.
- [38] M. Elsabahy, N. Wazen, N. Bayó-Puxan, G. Deleavey, M. Servant, M. J. Damha, J. C. Leroux, *Adv. Funct. Mater.* **2009**, *19*, 3862–3867.
- [39] D. J. Welsh, S. P. Jones, D. K. Smith, *Angew. Chem. Int. Ed.* **2009**, *48*, 4047–4051; *Angew. Chem.* **2009**, *121*, 4107–4111.
- [40] A. Mbarek, G. Moussa, J. L. Chain, *Molecules* **2019**, *24*, 1803.
- [41] W. Viricel, S. Poirier, A. Mbarek, R. M. Derbali, G. Mayer, J. Leblond, *Nanoscale* **2017**, *9*, 31–36.
- [42] W. Viricel, A. Mbarek, J. Leblond, *Angew. Chem. Int. Ed.* **2015**, *54*, 12743–12747; *Angew. Chem.* **2015**, *127*, 12934–12938.
- [43] J. Leblond, H. Gao, A. Petitjean, J. C. Leroux, *J. Am. Chem. Soc.* **2010**, *132*, 8544–8545.
- [44] Y. Xue, H. Bai, B. Peng, B. Fang, J. Baell, L. Li, W. Huang, N. H. Voelcker, *Chem. Soc. Rev.* **2021**, *50*, 4872–4931.
- [45] G. Leriche, L. Chisholm, A. Wagner, *Bioorg. Med. Chem.* **2012**, *20*, 571–582.
- [46] F. Kratz, I. A. Müller, C. Rypa, A. Warnecke, *ChemMedChem* **2008**, *3*, 20–53.
- [47] D. B. Rozema, A. V. Blokhin, D. H. Wakefield, J. D. Benson, J. C. Carlson, J. J. Klein, L. J. Almeida, A. L. Nicholas, H. L. Hamilton, Q. Chu, J. O.

- Hegge, S. C. Wong, V. S. Trubetskoy, C. M. Hagen, E. Kitas, J. A. Wolff, D. L. Lewis, *J. Controlled Release* **2015**, *209*, 57–66.
- [48] B. R. Meade, K. Gogoi, A. S. Hamil, C. Palm-Apergi, A. Van Den Berg, J. C. Hagopian, A. D. Springer, A. Eguchi, A. D. Kacsinta, C. F. Dowdy, A. Presente, P. Lönn, M. Kaulich, N. Yoshioka, E. Gros, X. S. Cui, S. F. Dowdy, *Nat. Biotechnol.* **2014**, *32*, 1256–1261.
- [49] C. Ma, D. Zhu, W. Lin, Y. Li, Y. Huang, H. Zhu, M. Ye, Y. Wang, L. Peng, X. Liu, *Chem. Commun.* **2022**, *58*, 4168–4171.
- [50] Y. Xiao, X. Tan, Z. Li, K. Zhang, *J. Mater. Chem. B* **2020**, *8*, 6697–6709.
- [51] J. Rautio, H. Kumpulainen, T. Heimbach, R. Oliyai, D. Oh, T. Järvinen, J. Savolainen, *Nat. Rev. Drug Discovery* **2008**, *7*, 255–270.
- [52] A. G. Gavriel, M. R. Sambrook, A. T. Russell, W. Hayes, *Polym. Chem.* **2022**, *13*, 3188–3269.
- [53] J. Geng, Y. Zhang, Q. Gao, K. Neumann, H. Dong, H. Porter, M. Potter, H. Ren, D. Argyle, M. Bradley, *Nat. Chem.* **2021**, *13*, 805–810.
- [54] J. A. Malla, V. K. Sharma, M. Lahiri, P. Talukdar, *Chem. Eur. J.* **2020**, *26*, 11946–11949.
- [55] S. Zhou, X. Hu, R. Xia, S. Liu, Q. Pei, G. Chen, Z. Xie, X. Jing, *Angew. Chem. Int. Ed.* **2020**, *59*, 23198–23205; *Angew. Chem.* **2020**, *132*, 23398–23405.
- [56] J. D. Bargh, S. J. Walsh, A. Isidro-Llobet, S. Omarjee, J. S. Carroll, D. R. Spring, *Chem. Sci.* **2020**, *11*, 2375–2380.
- [57] C. A. Blencowe, D. W. Thornthwaite, W. Hayes, A. T. Russell, *Org. Biomol. Chem.* **2015**, *13*, 8703–8707.
- [58] D. A. Roberts, B. S. Pilgrim, T. N. Dell, M. M. Stevens, *Chem. Sci.* **2020**, *11*, 3713–3718.
- [59] R. Kumari, M. M. Majumder, J. Lievonen, R. Silvennoinen, P. Anttila, N. N. Nupponen, F. Lehmann, C. A. Heckman, *Br. J. Cancer* **2021**, *124*, 1428–1436.
- [60] C. A. McGoldrick, Y. L. Jiang, V. Paromov, M. Brannon, K. Krishnan, W. L. Stone, *BMC Cancer* **2014**, *14*, 77.
- [61] S. Makherjee, R. N. Ghosh, F. R. Maxfield, *Physiol. Rev.* **1997**, *77*, 759–803.

Manuscript received: October 24, 2022

Accepted manuscript online: November 8, 2022

Version of record online: December 16, 2022